Bayesian inference of plastosphere viscosities near the Kunlun Fault, northern Tibet

G. E. Hilley,[1,2] R. Bürgmann,[1] P.-Z. Zhang,[3,4] and P. Molnar[5]

Received 1 October 2004; revised 19 November 2004; accepted 1 December 2004; published 5 January 2005.

[1] Flow of the mid-crust in the Tibetan Plateau may strongly influence the patterns of deformation and topography within this area. This flow requires the lower-crust to have low viscosity and so quantifying this viscosity may be used to test the idea of channel flow. An application of Bayesian methods to geologic and geodetic data from north central Tibet yields lower-crustal viscosities (assumed Newtonian) of 1×10^{19} Pa s and 2×10^{21} Pa s (95% bounds). The lower bound is larger than the value of 10^{16}–10^{18} Pa s required by models of flow of the lower-crust of Tibet, unless the entire lower crust participates in channel flow. **Citation:** Hilley, G. E., R. Bürgmann, P.-Z. Zhang, and P. Molnar (2005), Bayesian inference of plastosphere viscosities near the Kunlun Fault, northern Tibet, *Geophys. Res. Lett.*, *32*, L01302, doi:10.1029/2004GL021658.

1. Introduction

[2] Two simple views of continental deformation differ in how the upper crust and uppermost mantle are linked. In one case, the entire crust and mantle lithosphere deform by pure shear thickening, as implemented explicitly by the thin viscous sheet model [*Houseman and England*, 1986; *England and Houseman*, 1986]. In the other, the brittle upper crust is decoupled from the upper mantle, and in some cases deformation of the mid- to lower crust may occur by "channel flow" [*Royden et al.*, 1997; *Clark and Royden*, 2000; *Beaumont et al.*, 2004]. In the latter case, a low viscosity lower crust can mechanically decouple the crust from the mantle lithosphere, drastically altering the stresses and deformation in these types of continental orogens. Such channel flow has been proposed to explain the deformation within Tibet and topography around the margins of the Tibetan Plateau [e.g., *Clark and Royden*, 2000]. Because channel flow requires a low-viscosity zone in the mid- to lower crust, independent inferences of viscosity may be used to test the channel flow hypothesis. Herein, using geologic and geodetic data collected along and adjacent to the Kunlun Fault in northern Tibet, we show that the viscosity of the mid- to lower crust is at least approximately an order of magnitude larger than that required by most models of channel flow.

2. Methods

[3] We used geologic and geomorphic estimates of fault slip rates (9–16 mm/yr) and earthquake-rupture offsets in conjunction with geodetic data from northern Tibet (Figure 1) to estimate plastosphere viscosity and refine estimates of fault slip rate, schizosphere thickness, and recurrence time of events. Here, "schizosphere" refers to the portion of the upper crust that deforms elastically during interseismic periods, and "plastosphere" refers to areas that deform elastically over short time-scales but undergo viscous stress relaxation over longer time-scales [*Scholz*, 1988; *Savage*, 2000; *Dixon et al.*, 2003]. Assuming that the plastosphere deforms according to a Maxwell constitutive law [e.g., *Jaeger*, 1956], surface velocities observed during the earthquake-cycle may be used to estimate plastosphere viscosity [e.g., *Savage and Prescott*, 1978]. In the simplest view, the crust is idealized as two-dimensional in cross-section, so that movement along major strike-slip faults occurs in the out-of-plane dimension. The deformation during the earthquake cycle is defined by the long-term, average strike-slip rate of the modeled fault (s), the Maxwell relaxation time of the plastosphere ($\tau = 2\eta/\mu$, where η is the viscosity and μ is the shear modulus), the thickness of the schizosphere (H), the time since the last earthquake (t), and the average recurrence interval (T). Dimensional analysis reveals that four groups relate observed surface velocities to constitutive properties and rates of the schizo- and plastosphere [*Savage and Prescott*, 1978; *Segall*, 2002]: $t^* = t/T$, $\tau^* = \tau/T$, $s^* = s/s_{ref}$, and $H^* = H/x_{ref}$, where s_{ref} and x_{ref} are arbitrary slip-rate and length scales set to 1 mm/yr and 1 km, respectively. While simple, this model captures the basic observation that crustal deformation during the seismic cycle consists of coseismic elastic deformation followed by postseismic viscoelastic adjustment of the lower crust [e.g., *Savage and Prescott*, 1978; *Segall*, 2002] and has been successfully employed to provide first-order estimates of fault zone and lower-crustal properties in other regions [e.g., *Segall*, 2002]. It is important to acknowledge that the Kunlun Fault undergoes a left step ~250 km west of the geodetic profile, and continues eastward for another ~200 km. This discontinuity may violate some of the assumptions inherent in a two-dimensional model. In addition, the fault likely does not rupture along its entire 1600 km length in single events, and so three-dimensional effects of rupture along individual segments may lead to a slight overestimation of the plastosphere relaxation time.

[1]Department of Earth and Planetary Science, University of California, Berkeley, California, USA.
[2]Now at Department of Geological and Environmental Sciences, Stanford University, Stanford, California, USA.
[3]State Key Laboratory of Earthquake Dynamics, Institute of Geology, Chinese Earthquake Administration, Beijing, China.
[4]State Key Laboratory of Loess and Quaternary Geology, Institute of Earth Environment, Chinese Earthquake Administration, Beijing, China.
[5]Department of Geological Sciences and Cooperative Institute for Research in Environmental Sciences, University of Colorado, Boulder, Colorado, USA.

0094-8276/05/2004GL021658$05.00

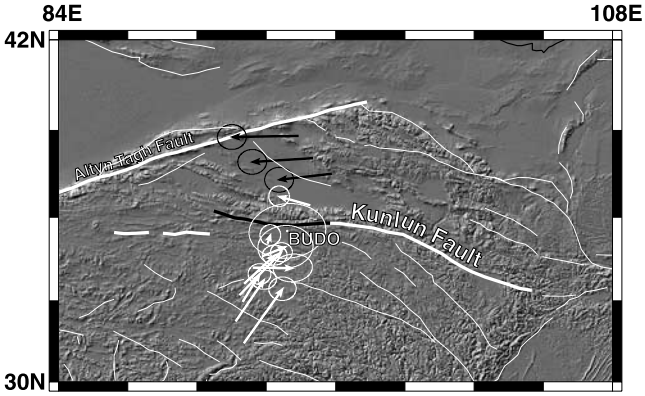

Figure 1. Location of the Kunlun Fault in northern Tibet, central Asia, and geodetic velocities used in this study. Error ellipses denote 95% confidence in velocities. Velocities are reported relative to station BUDO [*Zhang et al.*, 2004] (Figure 3). Velocities shown as solid white arrows were used to estimate plastosphere viscosities, while sites denoted by black arrows were not used due to their potential of recording the contraction taking place within the Qaidam basin and strike slip motion along the Altyn Tagh fault to the north. The black portion of the Kunlun Fault experienced a M 7.8 earthquake in 2001.

However, this model provides us with at least order-of-magnitude estimates of relaxation time (and hence plastosphere viscosity) for the region. Given the density of geodetic measurements from this portion of Tibet, the earthquake cycle modeling that we use allows us to glean information about plastosphere properties that otherwise could not be ascertained using the types of dislocation models currently employed to interpret interseismic geodetic velocities from this area [e.g., *Wallace et al.*, 2004; *Zhang et al.*, 2004].

[4] We incorporate geologic data and all sources of uncertainty into our viscosity estimates by exploiting Bayes' Rule [*Bayes*, 1763], which allows quantitative refinement of initial estimates of model parameters (in this case, fault zone and plastosphere properties) given the information provided by the geodetic observations [*Segall*, 2002; *Johnson and Segall*, 2004]:

$$P(m_i|x) = \frac{P(x|m_i)P(m_i)}{\sum_{j=1}^{n} P(x|m_j)P(m_j)} \quad (1)$$

where m_i denotes a vector of the four dimensionless model parameters, x is a vector of the normalized geodetic velocities observed, $P(m_i|x)$ denotes the probability that the set of model parameters explains the geodetic velocities, $P(x|m_i)$ is the probability of observing the geodetic velocities given a combination of model parameters m_i, and $P(m_i)$ is the probability that the chosen combination of model parameters actually occur. The denominator normalizes the probability to all possible combinations of model parameters. In this context, $P(x|m_i)$ encapsulates the goodness of fit between observed geodetic velocities and those that would be expected based on the viscoelastic model that relates the surface velocity distribution to fault-zone and plastosphere properties. $P(m_i)$ describes in a probabilistic sense, some prior knowledge about which sets of model parameters are likely to occur. This term may be used to incorporate information such as slip rates along faults and recurrence times of earthquakes whose range may be estimated based on geologic and geomorphic considerations [e.g., *Savage and Prescott*, 1978; *Buck et al.*, 1996; *Biasi et al.*, 2002]. To evaluate equation (1), we use the Metropolis-Hastings variant of the Markov-Chain Monte Carlo simulation methods that allows approximation of the joint distribution $P(m_i|x)$ without an exhaustive search of the parameter space [e.g., *Metropolis et al.*, 1953].

[5] With plausible ranges of t^*, τ^*, s^*, and H^* based on geologic, geomorphic, and seismological observations from the Kunlun fault (s = 9–16 mm/yr [*Kidd and Molnar*, 1988; *van der Woerd et al.*, 2002]; T covaries with s, given that coseismic offsets were observed to be 3.8–10 m [*Kidd and Molnar*, 1988; *van der Woerd et al.*, 2002; *Lin et al.*, 2002; *Xu et al.*, 2002]; t = 0–T; H = 12–26 km; τ = 0–600 yrs.), we used simple uniform probability distributions between the two reported extremes of each model parameter to construct the prior joint distribution, $P(m_i)$ (equation (1)). When we assign a wide range of values to t^*, we ignore the occurrence of the M 7.8 earthquake in 2001, which ruptured the Kunlun fault west of where the GPS line crosses the fault. Slip of ~2 m did occur in 2001 on a secondary fault, the Kunlun Pass fault, where the GPS line lies [*Lin et al.*, 2002; *Xu et al.*, 2002], but the main strand where 8–10 m offsets imply major past earthquakes [*Kidd and Molnar*, 1988; *van der Woerd et al.*, 2002] did not break in that event. We then used equation (1) to refine these initial estimates using the fault-parallel components of ten Global Positioning System (GPS) velocities along an ~600-km-long profile oriented approximately perpendicular to the strike of the fault [*Zhang et al.*, 2004]. Importantly, the velocities used in this study span the time period prior to the M7.8 2001 Kunlun earthquake, and so we expect no contamination in the velocities from coseismic displacements during this event. We excluded sites located far to the north of the Kunlun fault to avoid the potentially confounding effects of slip along contractional and strike slip faults in those areas.

3. Results

[6] Values of s^* = 10.2, t^* = 0.37, τ^* = 0.0338, and H^* = 12.5 yielded the highest probability in the joint probability density function (pdf) (Figures 2 and 3 and Table 1) and lie within the extremes of the probable model parameter values based on their marginal distributions (Figures 2a–2c). Marginal distributions of these groups show a positively skewed s^* marginal probability density (mpdf; Figure 2a), a negatively skewed t^* mpdf (Figure 2b), and an approximately log-normally distributed τ^* mpdf (Figure 2c). Increasing s^* requires decreasing τ^* (Figure 2d), increasing t^* requires increasing τ^* (Figure 2e), and increasing H^* requires increases in t^* (Figure 2f), although covariance between the latter set of dimensionless groups is small. The non-linearity of the simple viscoelastic model allows complex model behavior that results in a myriad of trade-offs between the different variables, and this sometimes allows

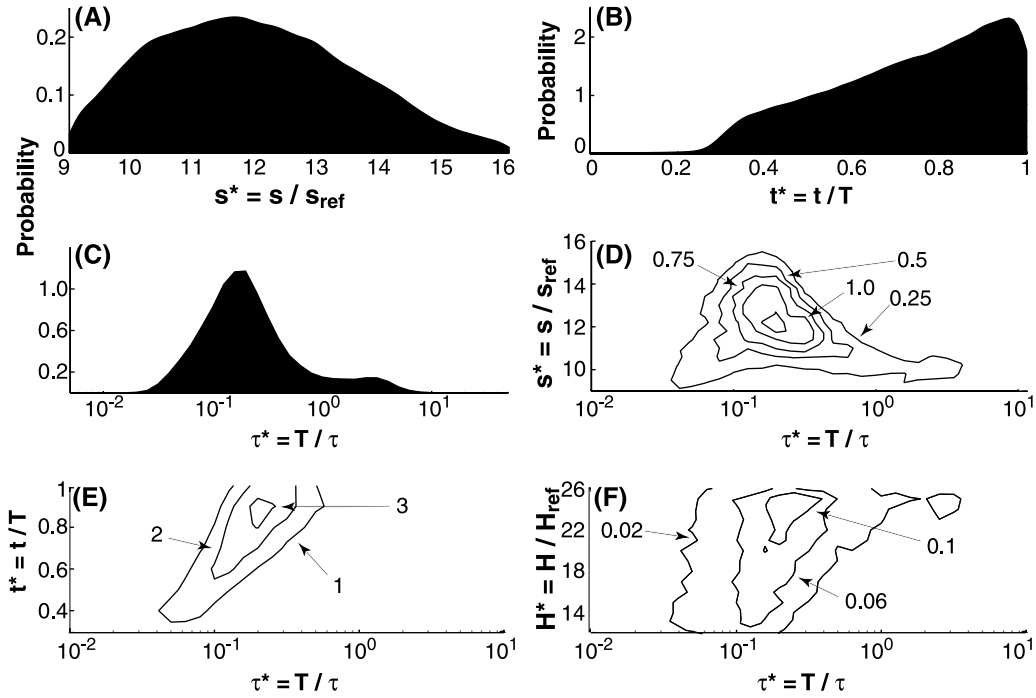

Figure 2. (a–c) Parameter estimates for s*, t*, and τ* inferred from Bayesian analysis. (d–f) Marginal distributions, which collapse the joint pdf onto a subset of model parameter dimensions, show covariation of τ* with s*, t*, and H*, respectively.

the optimum value (which is only weakly favored over other model parameter combinations) to lie outside of the 95% bounds of the model parameter value. The measured components of velocity and simulated predictions (Figure 3) agree within uncertainties of measurements. The nonlinearity of the viscoelastic model permits a plethora of trade-offs between model parameters that allow the optimal velocity profile to lie outside of the 1σ predicted range.

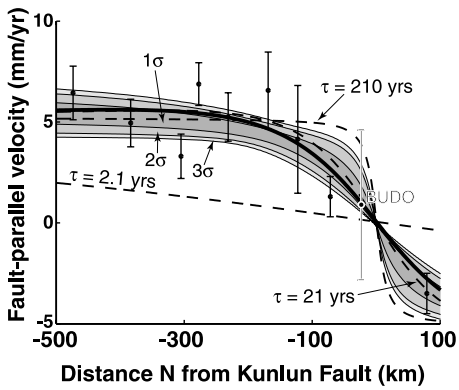

Figure 3. Observed fault-parallel velocity profile (dots with error bars) and range of profiles generated by Monte Carlo simulations (shaded areas). Heavy solid line shows best-fitting calculated profile. Dashed lines show velocity profiles that result from optimal values of s^*, H^*, and t*, assuming that $T = 500$ years. This value of T was chosen to produce the steepest possible velocity gradients (and hence, the best fit to the observed velocity profile when plastosphere viscosity is low) that would be expected for plastosphere relaxation times of $\tau = 211$ yrs (1×10^{20} Pa s), 21.1 yrs (1×10^{19} Pa s), and 2.1 years (1×10^{18} Pa s).

Coseismic ruptures observed over several earthquake cycles along the main strand of the Kunlun Fault consistently produce 8–10 m of strike-slip offset during each event [*Kidd and Molnar*, 1988; *van der Woerd et al.*, 2002], and the estimated range in the fault's slip rate (9–16 mm/yr [*Kidd and Molnar*, 1988; *van der Woerd et al.*, 2002]) implies an average earthquake recurrence time of 500–1111 years. Using this range and assuming a shear modulus of 30 GPa, our estimates of τ* imply plastosphere viscosities between 1×10^{19} Pa s and 2×10^{21} Pa s (95% bounds). Accordingly, velocity profiles expected for viscosities of 1×10^{20}, 1×10^{19}, and 1×10^{18} Pa s, respectively (Figure 3), indicate that viscosities $<1 \times 10^{18}$ Pa s ($\tau < 2.1$ years) would lead to exceedingly small surface velocity gradients. In the context of linear viscosity, if these low values apply to geologic time-scales, geodetically observed deformation should be extremely broad [*Savage and Prescott*, 1978] and would likely span the entire width of the Tibetan plateau rather than being expressed as persistent, resolvable velocity changes across major fault zones [*Wallace et al.*, 2004; *Zhang et al.*, 2004].

4. Discussion and Conclusions

[7] Numerical simulations that consider the effects of a weak mid- to lower-crust underlain by a strong lithospheric

Table 1. Summary Statistics of Inferred Model Parameter Values, Considering Geologic, Geomorphic and Geodetic Data

	Optimal Value	Mean	Median	σ	95% Bounds
s^*	10.2	11.9	11.8	1.5	9.3–15.1
t^*	0.37	0.74	0.77	0.2	0.31–0.98
τ^*	0.0338	0.446	0.187	0.829	0.04–3.25
H^*	12.5	20.3	20.9	3.9	12.6–25.8

mantle [*Hetland and Hager*, 2004] indicate that interseismic velocities reflect the viscosity of the weak lower crust, rather than the strong lithospheric mantle. Therefore, our viscosity estimates should reflect the viscosity of the lower crust, even in the presence of a strong upper mantle. In contrast to our inferred viscosities, estimates of Tibetan lower-crustal viscosity based on topographic gradients [*Clark and Royden*, 2000] and geodynamic models [*Shen et al.*, 2001] are 10^{16} Pa s and 10^{18} Pa s, respectively, supposing that a weak, mid-crustal channel is 15 km thick. Because these previous viscosity estimates scale with the cube of the assumed channel thickness, our viscosities would require channel thickness values between 147–832 km (95% bounds) for viscosities inferred from topographic gradients [*Clark and Royden*, 2000] and 32–179 km (95% bounds) for viscosities inferred from geodynamic modeling [*Shen et al.*, 2001]. Recent seismological observations from southern and western Tibet indicate that the mantle lithosphere may be strong [*Chen and Yang*, 2004], suggesting that crustal channel thickness may not exceed 90 km. Despite the wide range of viscosities allowed by our model, when applied to those previously estimated using topographic gradients [*Clark and Royden*, 2000], our viscosities require channels that penetrate the entire lithosphere. If so, at least in the central northern Tibetan plateau, topography does not appear to serve as a reliable proxy for lower-crustal viscosity. On the other hand, when our viscosities are applied to geodynamic models of lower-crustal channel flow that address other aspects of Asian geology [*Shen et al.*, 2001], more plausible, yet larger channel thicknesses than previously considered (>30 km) are consistent with our lowermost bounds on estimated viscosity. It is possible that a power-law constitutive relationship may, in some cases, reconcile the relatively large viscosity that we infer with the presence of lower-crustal channel flow [*Beaumont et al.*, 2004], and so we cannot rule out the possibility that a lower-crustal channel may be present beneath northern Tibet within the 95% bounds of our estimates. In any case, our viscosity estimates indicate that if a lower-crustal channel exists beneath northern Tibet, it must be thicker than previously thought. However, the range in viscosity estimates favoured by our analysis appears more compatible with a scenario in which the upper crust is mechanically linked to the uppermost mantle through a viscous mid- to lower-crust.

[8] **Acknowledgments.** We thank J. Savage for a review of an earlier draft of this manuscript and J. Chery and G. Houseman for helpful reviews that improved this paper. This research was supported in part by the National Science Foundation under grant EAR-0003449. BSL Contribution # 05-01.

References

Bayes, T. (1763), An essay towards solving a problem in the doctrine of chances, *Philos. Trans. R. Soc. London*, *53*, 370–418.

Beaumont, C., R. A. Jamieson, M. H. Nguyen, and S. Medvedev (2004), Crustal channel flows: 1. Numerical models with applications to the tectonics of the Himalayan-Tibetan orogen, *J. Geophys. Res.*, *109*, B06406, doi:10.1029/2003JB002809.

Biasi, G. P., R. J. Weldon II, T. E. Fumal, and G. G. Seitz (2002), Paleoseismic event dating and the conditional probability of large earthquakes on the southern San Andreas fault, California, *Bull. Seismol. Soc. Am.*, *92*, 2761–2781.

Buck, C. E., W. G. Cavanagh, and C. D. Litton (1996), *The Bayesian Approach to Interpreting Archaeological Data*, 382 pp., John Wiley, Hoboken, N. J.

Chen, W.-P., and Z. Yang (2004), Earthquakes beneath the Himalayas and Tibet: Evidence for a strong lithospheric mantle, *Science*, *304*, 1949–1952.

Clark, M. K., and L. H. Royden (2000), Topographic ooze: Building the eastern margin of Tibet by lower crustal flow, *Geology*, *28*, 703–706.

Dixon, T. H., E. Norabuena, and L. Hotaling (2003), Paleoseismology and Global Positioning System: Earthquake-cycle effects and geodetic versus geologic fault slip rates in the eastern California shear zone, *Geology*, *31*, 55–58.

England, P. C., and G. A. Houseman (1986), Finite strain calculations of continental deformation: 2. Comparison with the India-Asia collision zone, *J. Geophys. Res.*, *91*, 3664–3676.

Hetland, E. A., and B. H. Hager (2004), Relationship of geodetic velocities to velocities in the mantle, *Geophys. Res. Lett.*, *31*, L17604, doi:10.1029/2004GL020691.

Houseman, G. A., and P. C. England (1986), Finite strain calculations of continental deformation: 1. Method and general results for convergent zones, *J. Geophys. Res.*, *91*, 3651–3663.

Jaeger, J. C. (1956), *Elasticity, Fracture, and Flow*, Methuen, New York.

Johnson, K. M., and P. Segall (2004), Viscoelastic earthquake cycle models with deep stress-driven creep along the San Andreas fault system, *J. Geophys. Res.*, *109*, B10403, doi:10.1029/2004JB003096.

Kidd, W. S. F., and P. Molnar (1988), Quaternary and active faulting observed on the 1985 Academia Sinica–Royal Society geotraverse of Tibet, *Philos. Trans. R. Soc. London*, *327*, 337–363.

Lin, A., B. Fu, J. Guo, Q. Zeng, G. Dang, W. He, and Y. Zhao (2002), Coseismic strike-slip and rupture length produced by the 2001 M_s 8.1 central Kunlun earthquake, *Science*, *296*, 2015–2017.

Metropolis, N., A. W. Rosenbluth, M. N. Rosenbluth, A. H. Teller, and E. Teller (1953), Equations of state calculations by fast computing machines, *J. Chem. Phys.*, *21*, 1087–1091.

Royden, L. H., B. C. Burchfiel, R. W. King, E. Wang, Z. Chen, F. Shen, and Y. Liu (1997), Surface deformation and lower crustal flow in eastern Tibet, *Science*, *276*, 788–790.

Savage, J. C., and W. H. Prescott (1978), Asthenosphere readjustment and the earthquake cycle, *J. Geophys. Res.*, *83*, 3369–3376.

Savage, J. C. (2000), Viscoelastic-coupling model for the earthquake cycle driven from below, *J. Geophys. Res.*, *105*, 25,525–25,532.

Scholz, C. H. (1988), *The Mechanics of Earthquakes and Faulting*, Cambridge Univ. Press, New York.

Segall, P. (2002), Integrating geologic and geodetic estimates of slip rate on the San Andreas fault system, *Int. Geol. Rev.*, *44*, 62–82.

Shen, F., L. H. Royden, and B. C. Burchfiel (2001), Large-scale crustal deformation of the Tibetan Plateau, *J. Geophys. Res.*, *106*, 6793–6816.

van der Woerd, J., P. Tapponnier, F. J. Ryerson, A.-S. Meriaux, B. Meyer, Y. Gaudemer, R. C. Finkel, M. W. Caffee, G. Zhao, and Z. Xu (2002), Uniform postglacial slip-rate along the central 600 km of the Kunlun Fault (Tibet), from ^{26}Al, ^{10}Be, and ^{14}C dating of riser offsets, and climatic origin of the regional morphology, *Geophys. J. Int.*, *148*, 356–388.

Wallace, K., G. Yin, and R. Bilham (2004), Inescapable slow slip on the Altyn Tagh fault, *Geophys. Res. Lett.*, *31*, L09613, doi:10.1029/2004GL019724.

Xu, X., W. Chen, W. Ma, G. Yu, and G. Chen (2002), Surface rupture of the Kunlunshan earthquake (M_s 8.1), northern Tibetan Plateau, China, *Seismol. Res. Lett.*, *73*, 884–892.

Zhang, P. Z., et al. (2004), Continuous deformation of the Tibetan Plateau from GPS, *Geology*, *32*, 809–812.

R. Bürgmann and G. E. Hilley, Department of Earth and Planetary Science, University of California, 377 McCone Hall, Berkeley, CA 94720-4767, USA. (hilley@pangea.stanford.edu)

P. Molnar, Department of Geological Sciences and Cooperative Institute for Research in Environmental Sciences, University of Colorado, Boulder, CO 80309, USA.

P.-Z. Zhang, State Key Laboratory of Earthquake Dynamics, Institute of Geology, Chinese Earthquake Administration, Beijing 100029, China.